Isolation and Strain-Specific Characterization of Pathogenic CJD Prion Particles

Dr. Leonardo Cortez

July 14th, 2018

UNIVERSITY OF ALBERTA

CENTRE FOR PRIONS
AND PROTEIN FOLDING DISEASES

Prion protein (PrP) and Prion disease

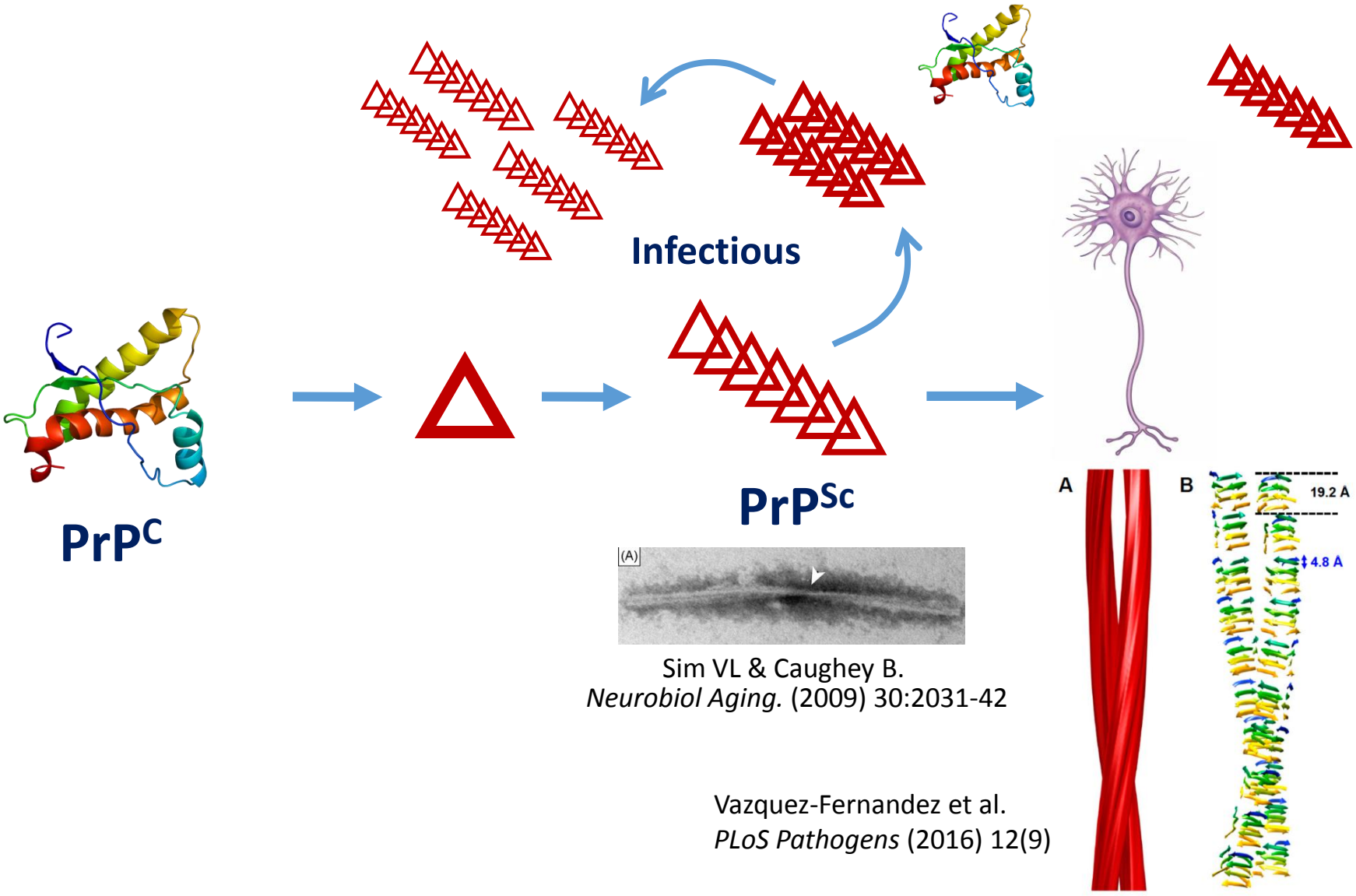

Sim VL & Caughey B.
Neurobiol Aging. (2009) 30:2031-42

Vazquez-Fernandez et al.
PLoS Pathogens (2016) 12(9)

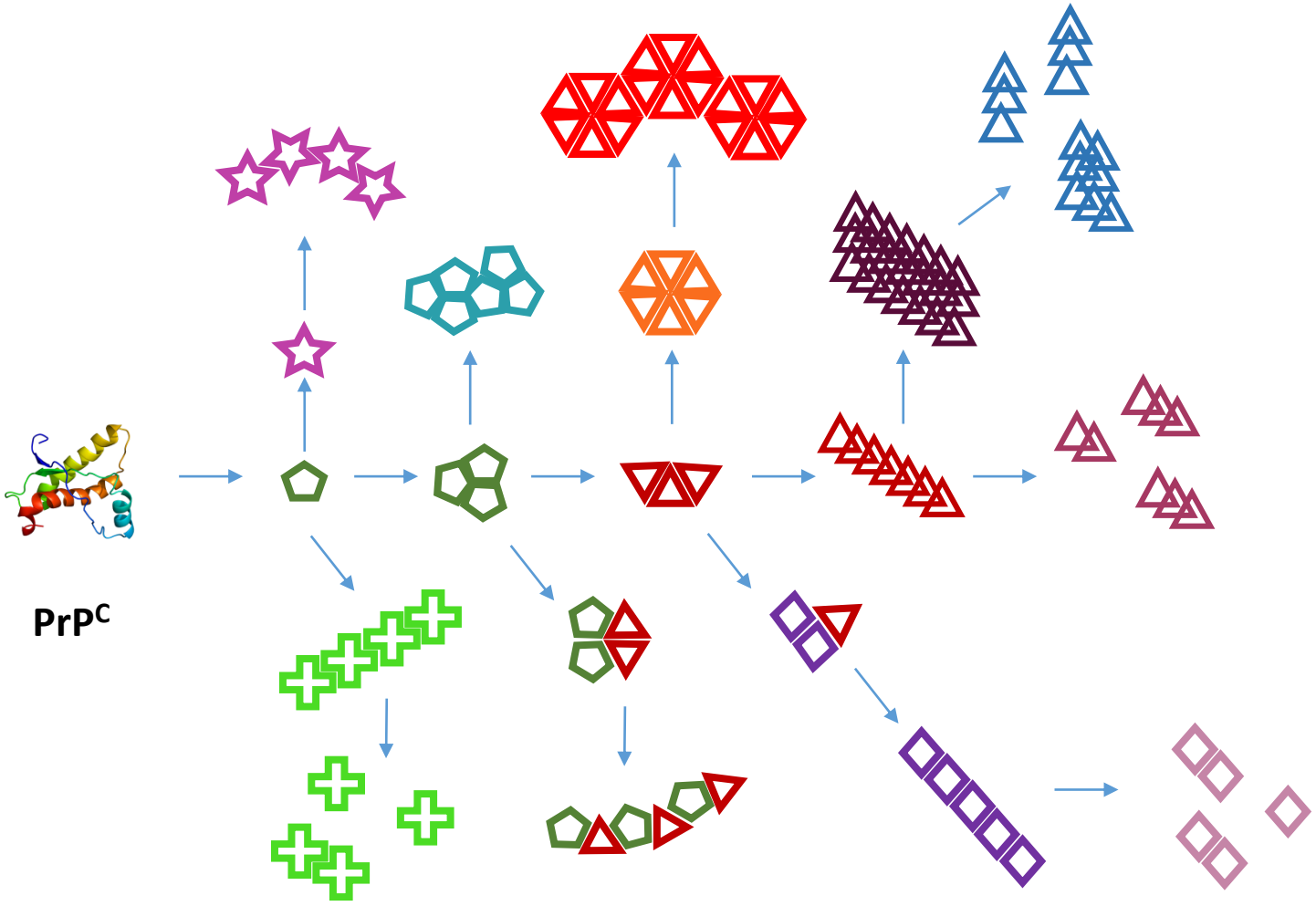
PrP^C

PrP^C

PrP^C

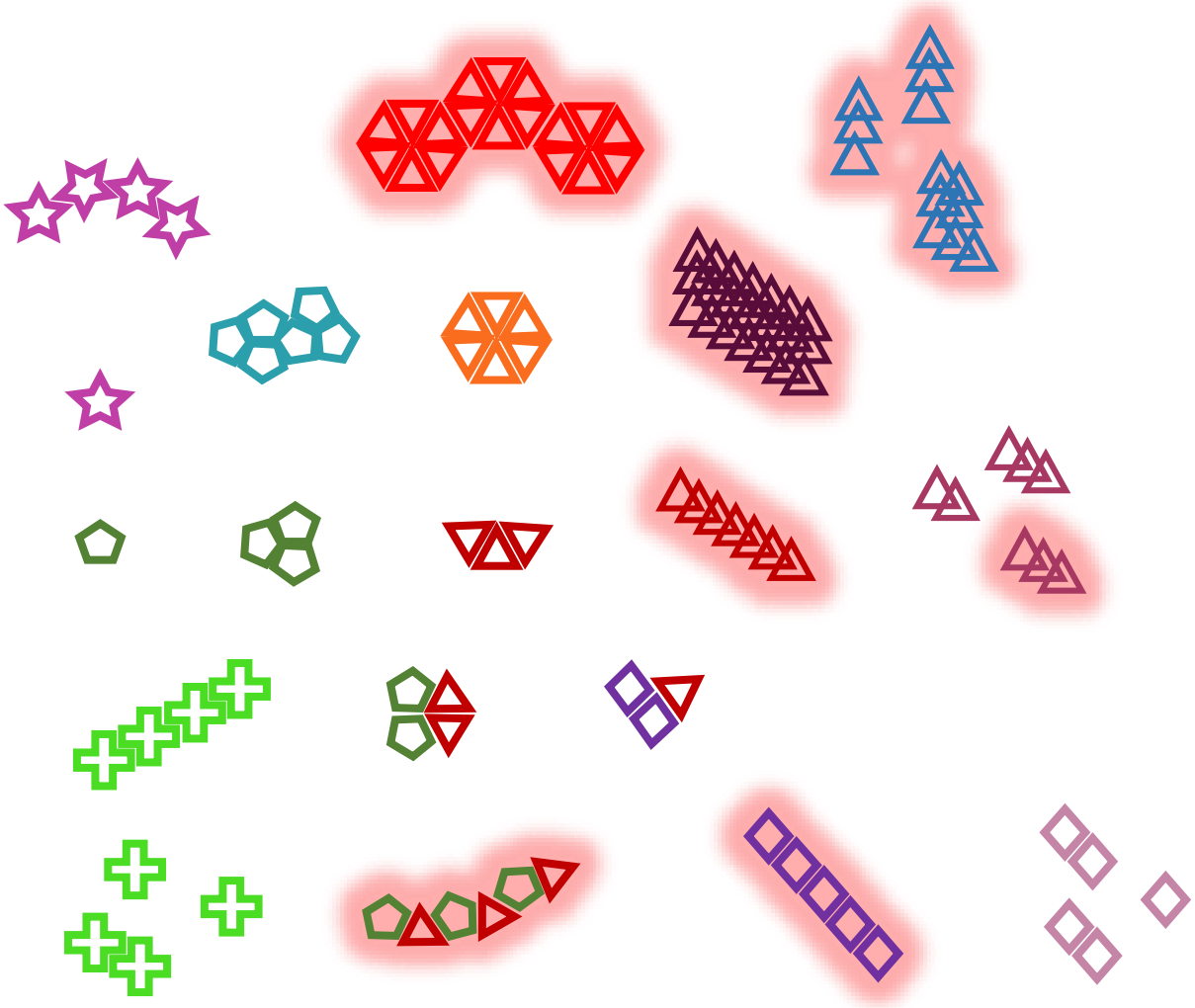

PrP^C

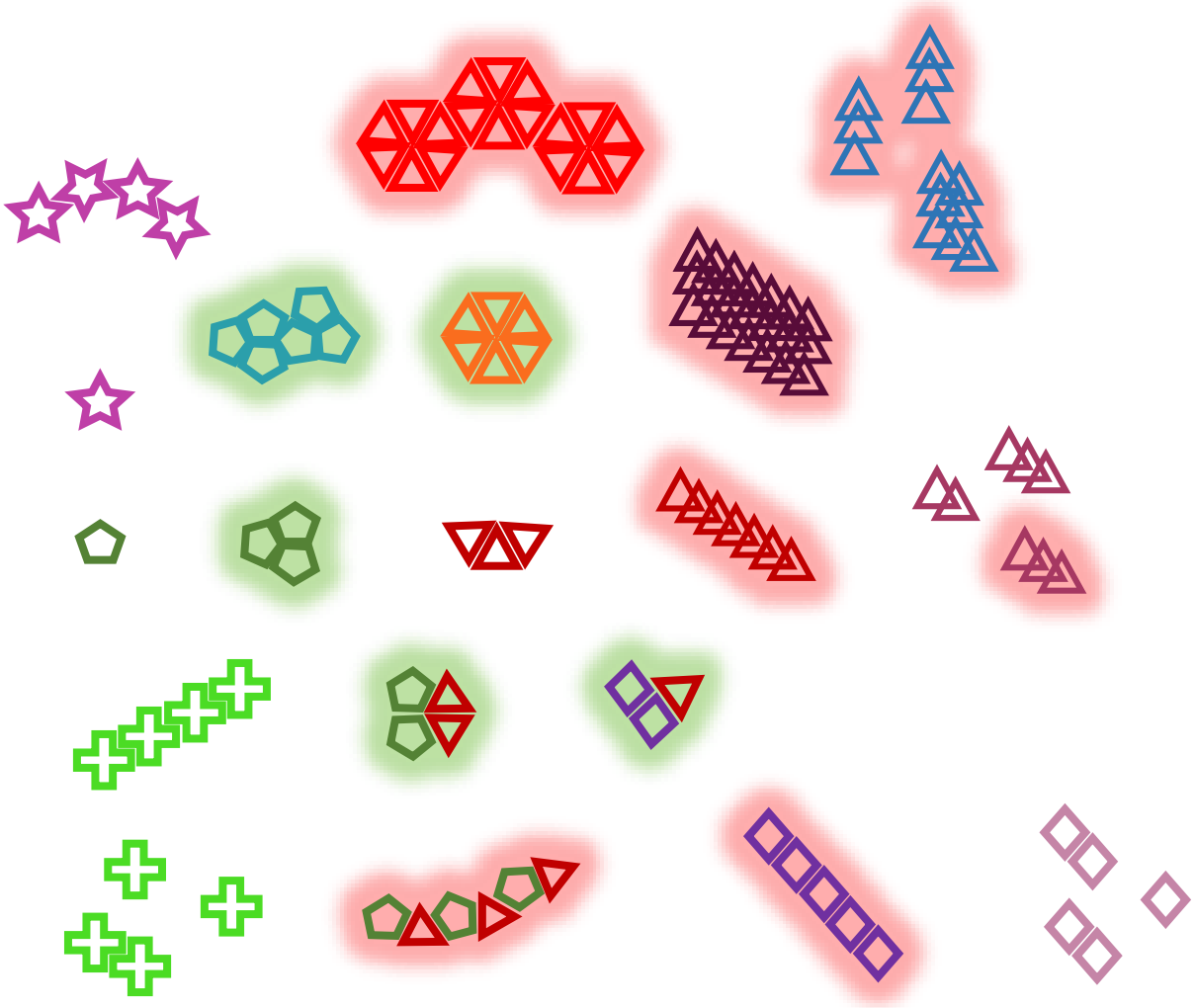

Strain cloud

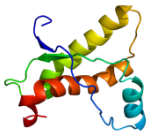

PrP^{C}

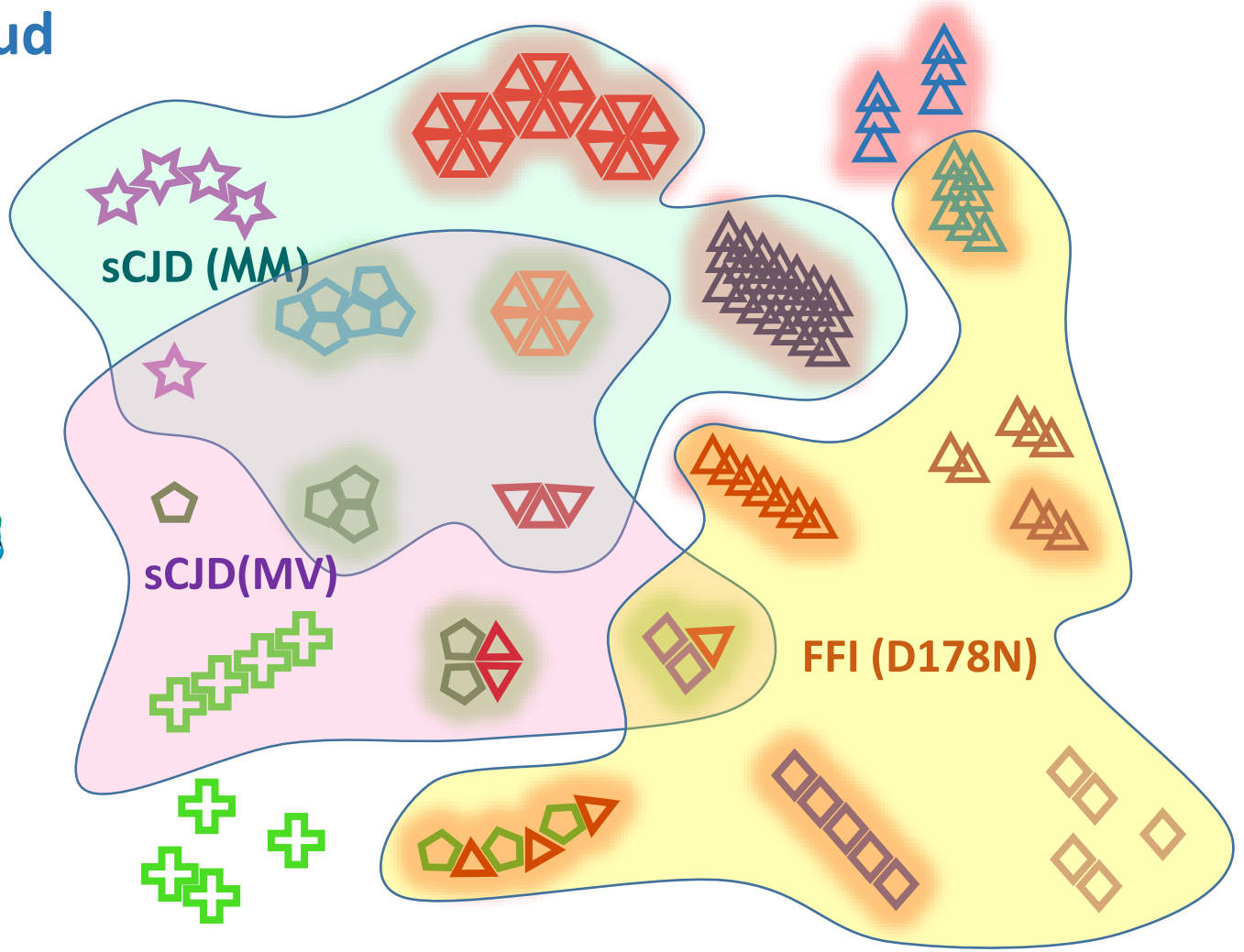

- Can we isolate the different prion particles present in brains at terminal stage of prion disease?
- Are different strains composed by different cloud of prion particles?
- Can we characterize the prion particles present in these clouds and identify the most pathogenic prions?
- Are these pathogenic particles strain-specific?

10% Brain homogenate

↓

Solubilisation

1) **2% dodecyl maltoside, 30 min, 4ºC**
2) **2% sarkosyl, 30 min, 4ºC**

↓

Centrifugation

20,000rpm, 10min, 4°C

Supernatant | **Pellet**

↓

80µL injected in AF4

Running buffer: 50mM HEPES, 135mM NaCl, 0.05% SDS; pH 7.4

↓

Western blot (primary antibody SAF83 1:3000)

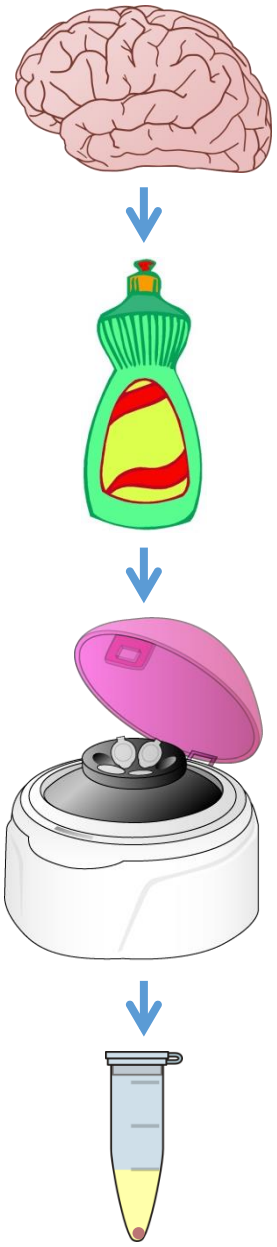

Tixador et al. *PLoS Pathog.* 2010; 6(4).

Asymmetric-Flow Field-Flow Fractionation (AF4)

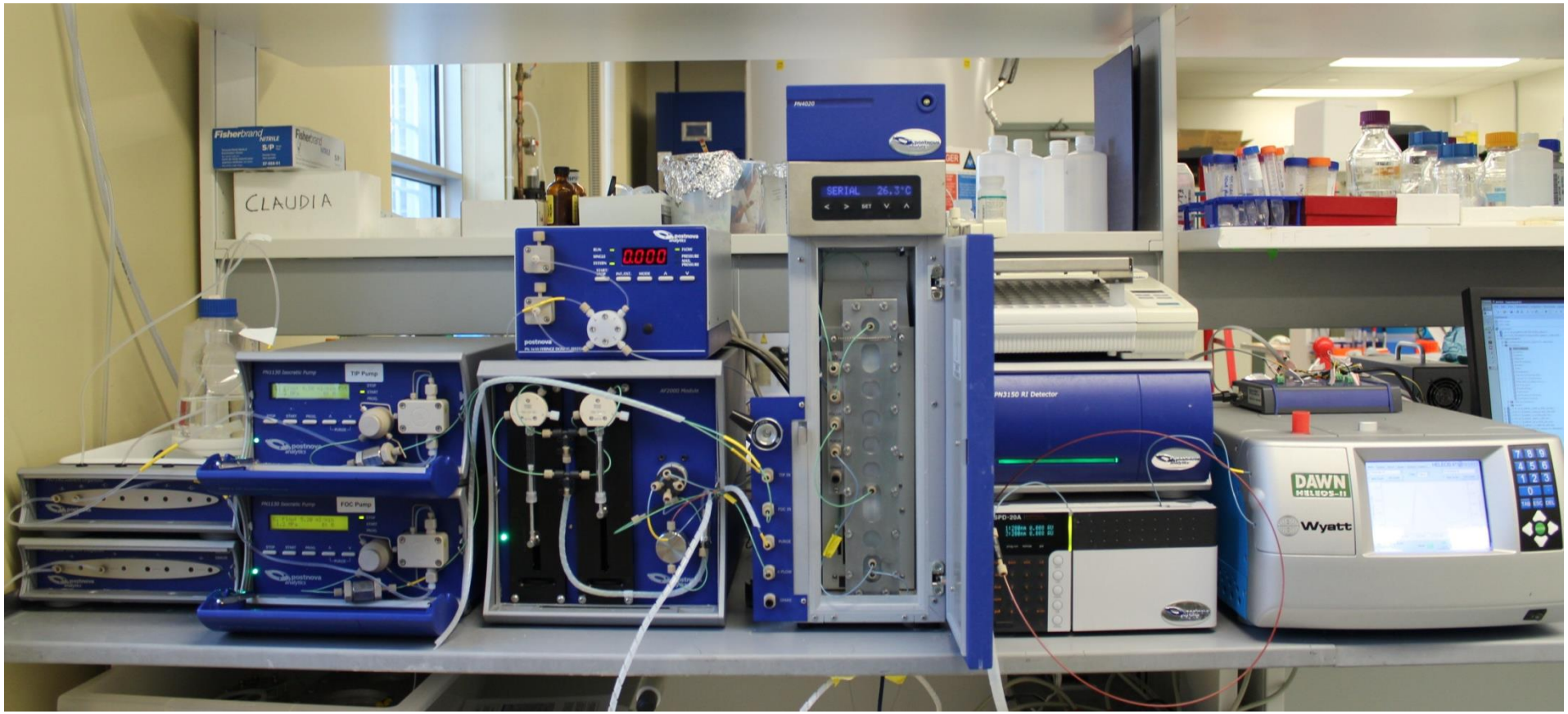

Asymmetric-flow field-flow fractionation (AF4)

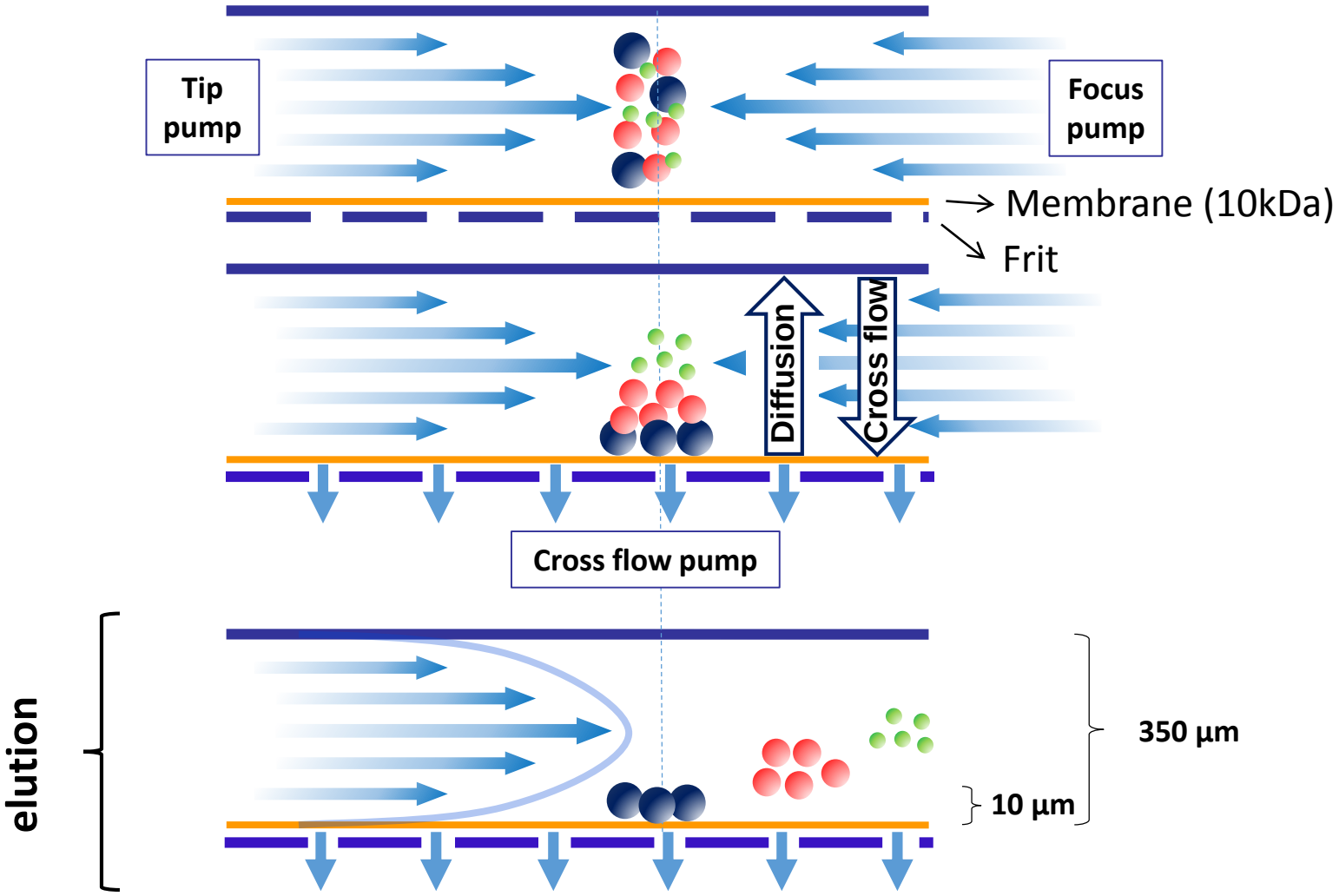

Asymmetric-flow field-flow fractionation (AF4)

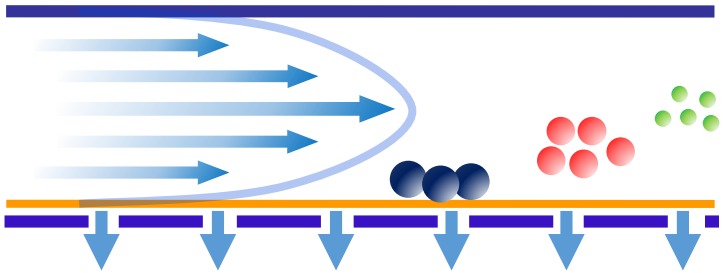

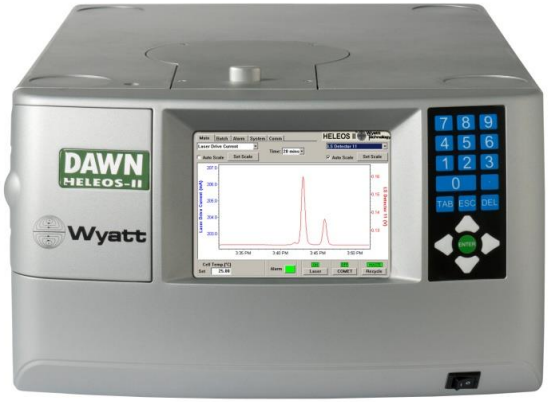

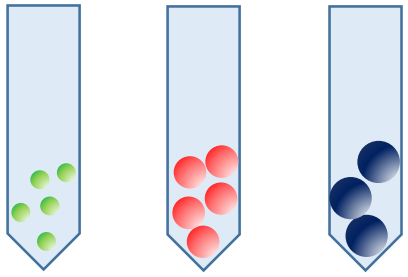

Fraction # 1 2 3

Dynamic Light Scattering (DLS)

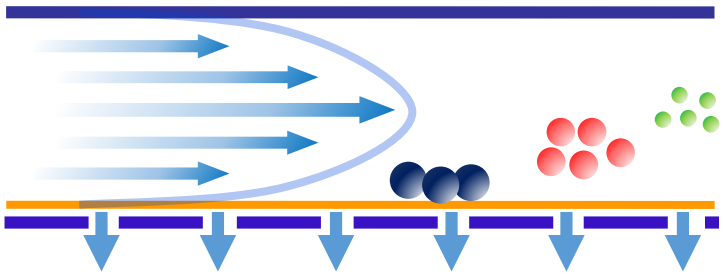

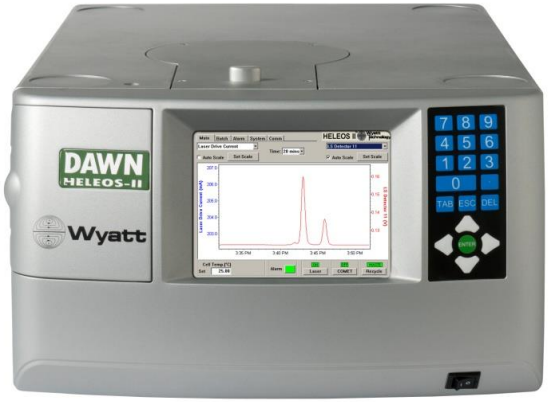

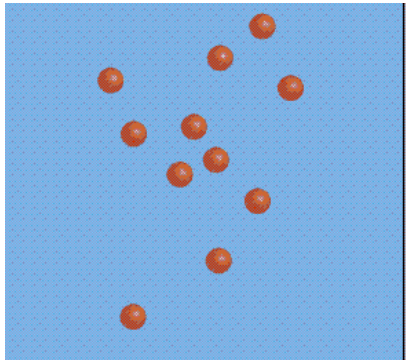

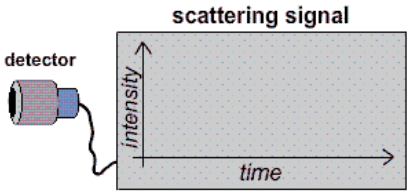

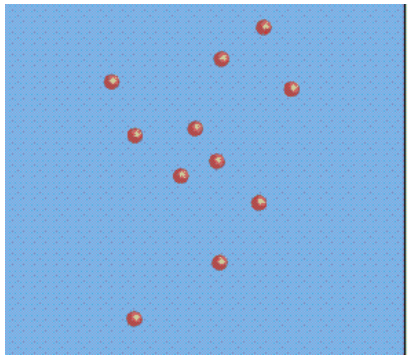

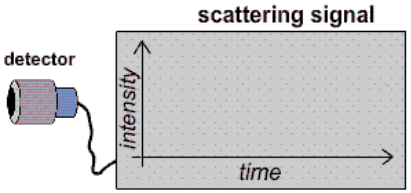

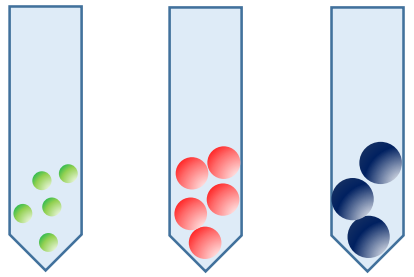

Fraction #	1	2	3
R_H	+	+++	+++++

Immunoblotting

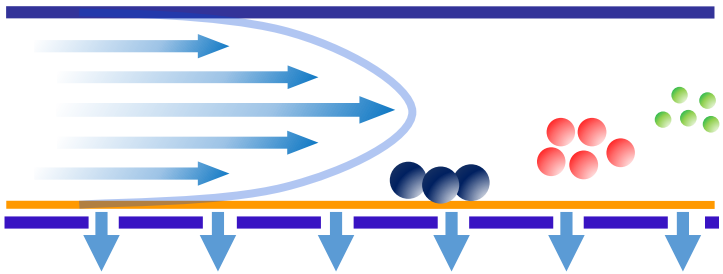

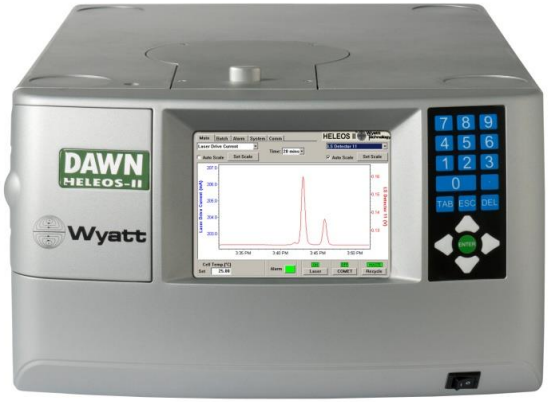

Fraction # 1 2 3

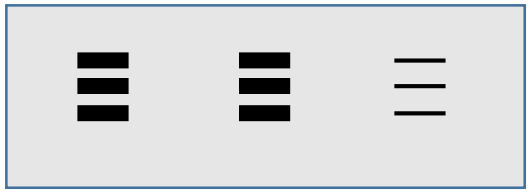

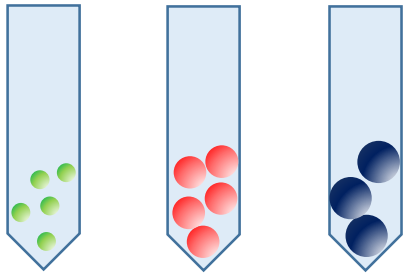

Fraction #	1	2	3
R_H	+	+++	+++++
Amount	+++	+++	+

PrP size distribution

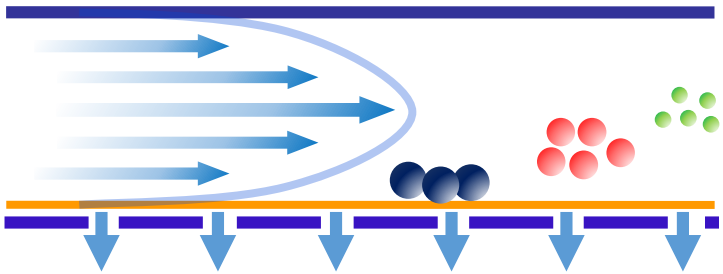

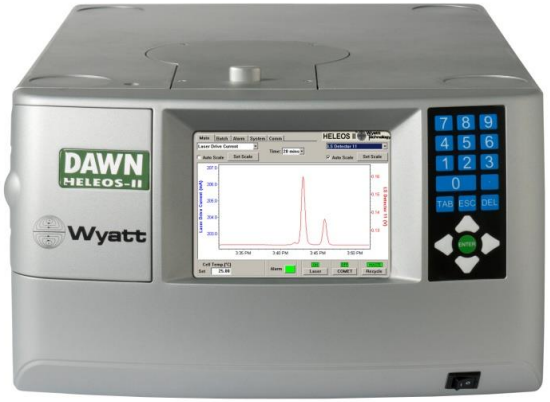

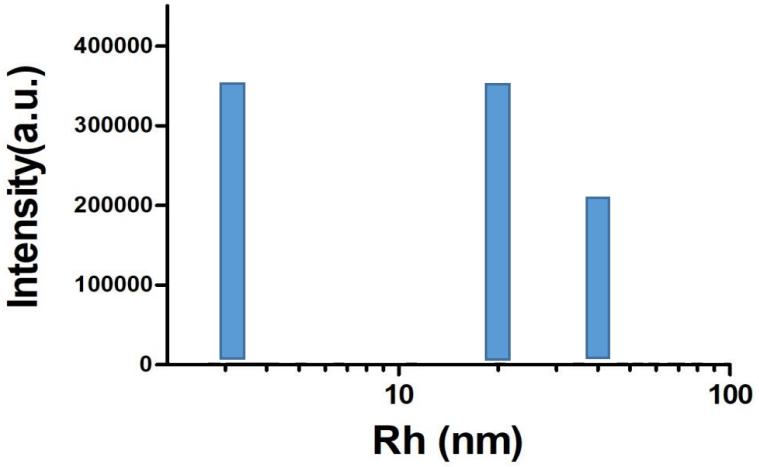

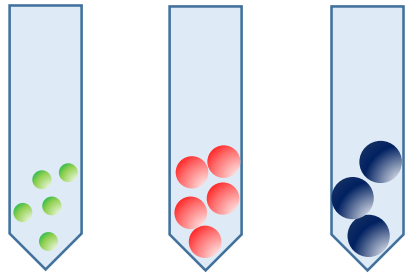

Fraction #	1	2	3
R_H	+	+++	+++++
Amount	+++	+++	+

Mouse prion strains

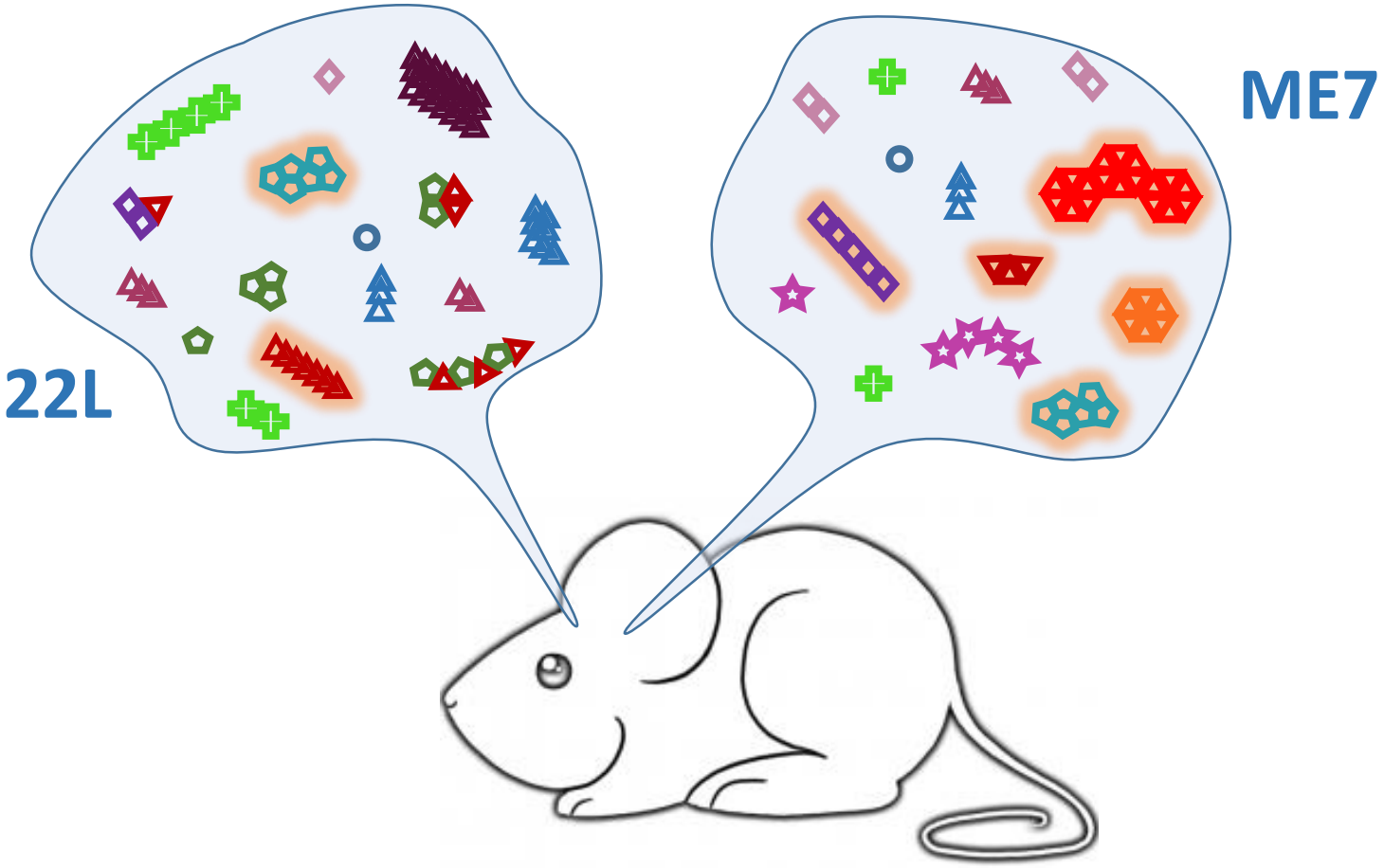

Table 2. *Mean incubation period for different combinations of scrapie strain and mouse strain or cross*

Route of infection	Scrapie strain	Mean incubation period (days) ± S.E.M. VM	C57BL	VM × C57BL	VM-*Sinc*^{s7}	VM × VM-*Sinc*^{s7}
I.c. (previous data)	ME7	328 ± 4(14)*	171 ± 2(16)	251 ± 2(12)		
	22C	458 ± 3(11)	182 ± 1(18)	269 ± 4(16)		
	22L	208 ± 1(16)	148 ± 1(17)	189 ± 1(17)		

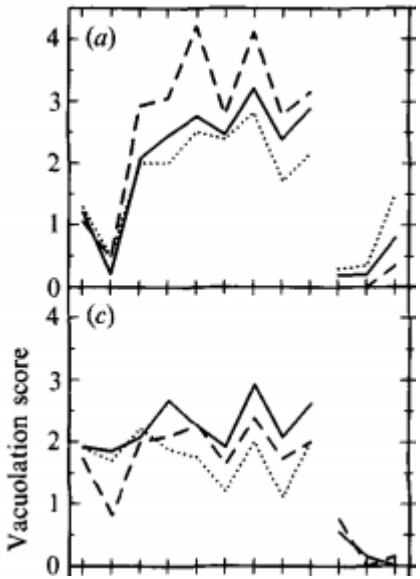

Fig. 5. Lesion profiles for six strains of scrapie injected i.c. into VM-*Sinc*^{s7} (——), VM (– – –) and C57BL (···) mice (n = eight to 25 mice/group). Mice were injected with (*a*) ME7, (*b*) 22C, (*c*) 22L, (*d*) 79A, (*e*) 139A and (*f*) 22A. Vacuolar degeneration was scored in nine grey matter and three white matter areas of brain (Fraser & Dickinson, 1968; Fraser, 1976). The grey matter areas are: 1, dorsal medulla; 2, cerebellar cortex; 3, superior colliculus; 4, hypothalamus; 5, medial thalamus; 6, hippocampus; 7, septum; 8, medial cerebral cortex at the level of the thalamus; 9, medial cerebral cortex at the level of the septum. The white matter areas are 1*, cerebellar white matter; 2*, white matter of the mesencephalic tegmentum; 3*, pyramidal tract.

Bruce et al. *J. Gen. Virol.* (1991), 72, 595-603

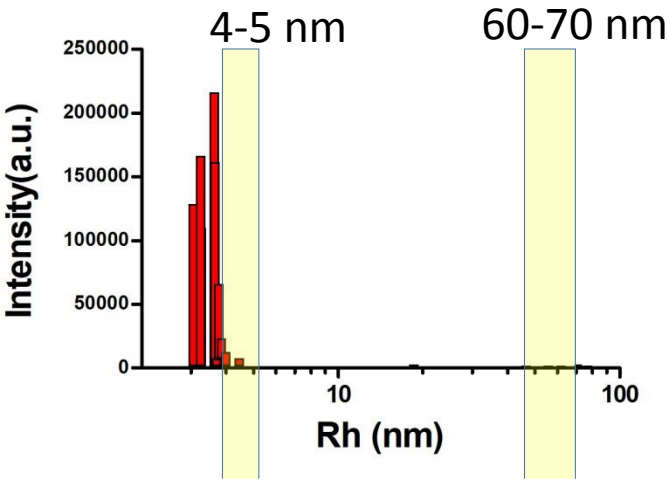

NBH

Globular protein

4-5 nm
86-132 kDa
3-5-mer PrP particles

Fibrillar structure ?

60-70 nm

Hamster prion strains

263K

Hyper

Drowsy

Table 1. Properties of hamster-adapted prion strains.

	Incubation period (days)		PrP^{Sc} properties					
Strain	**i.c.**	**i.sc.**	**Migration**	**$[Gdn\text{-}HCl]_{1/2}$**	**$[SDS]_{1/2}$**	**Amplification coefficient**	**Source**	**Ref.**
HY TME	65±3[a]	70±3	21 kDa	1.16±0.09	1.14±0.03	20	TME	[58]
263K	61±3	72±3	21 kDa	1.57±0.02	1.04±0.06	20	Scrapie	[62]
HaCWD	61±3	73±3	21 kDa	1.27±0.09	0.78±0.02	2	CWD	[63]
22AH	136±5	n.d.	21 kDa	1.02±0.02	0.53±0.04	0.02	Scrapie	[64]
22CH	161±3	n.d.	21 kDa	0.67±0.02	0.46±0.02	0.02	Scrapie	[64]
139H	159±3	198±3	21 kDa	0.76±0.05	0.50±0.01	0.02	Scrapie	[64]
DY TME	170±4	235±3	19 kDa	0.43±0.03	0.53±0.05	0.02	TME	[58]
ME7H	263±3	n.d.	21 kDa	0.59±0.03	0.44±0.02	0.02	Scrapie	[64]

[a]Mean ± SEM, n = 5.
n.d. – not done.
doi:10.1371/journal.ppat.1001317.t001

Ayers et al. (2011) *PLoS Pathog* 7(3): e1001317

Drowsy

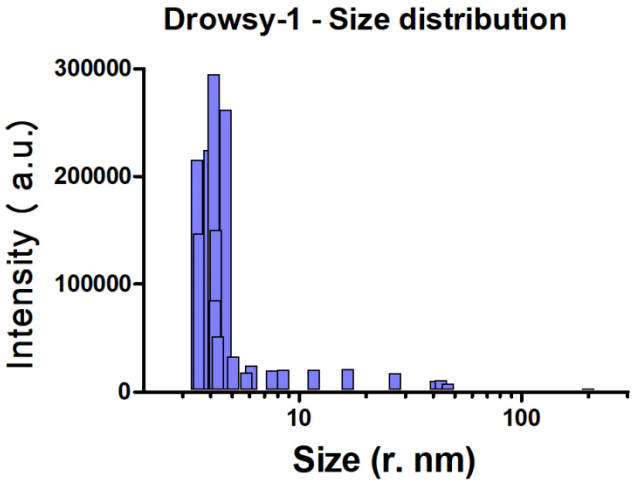
Drowsy-1 - Size distribution
Intensity (a.u.)
300000
200000
100000
0
10
100
Size (r. nm)

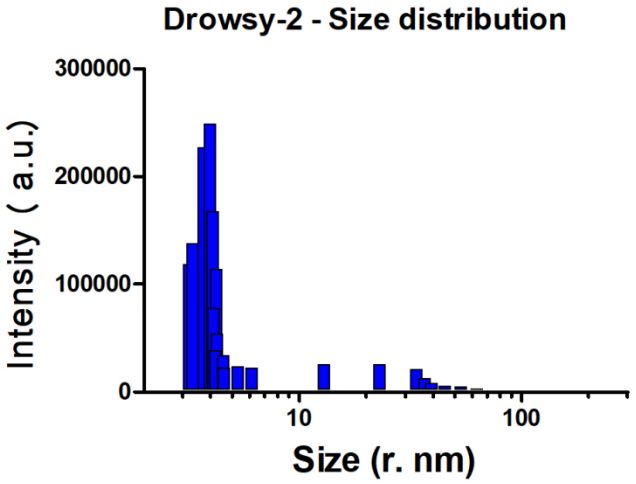
Drowsy-2 - Size distribution
Intensity (a.u.)
300000
200000
100000
0
10
100
Size (r. nm)

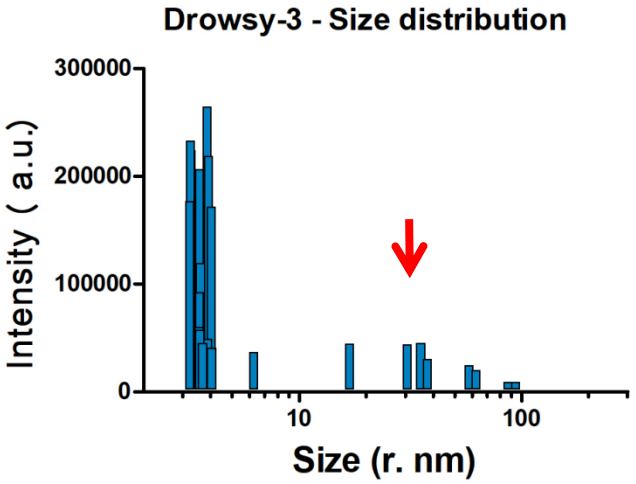
Drowsy-3 - Size distribution
Intensity (a.u.)
300000
200000
100000
0
10
100
Size (r. nm)

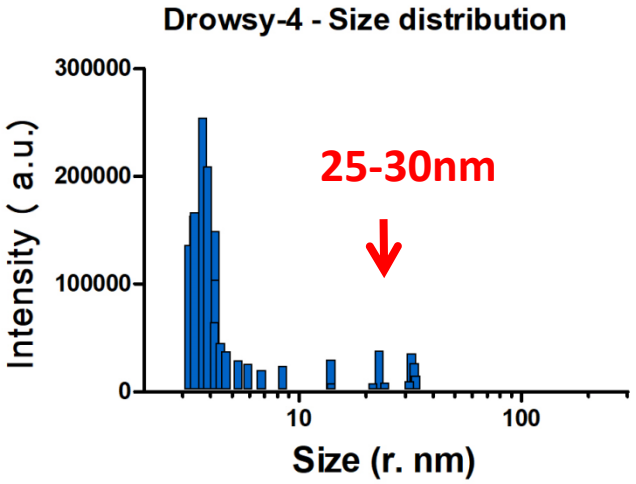
Drowsy-4 - Size distribution
Intensity (a.u.)
300000
200000
100000
0
25-30nm
10
100
Size (r. nm)

263K

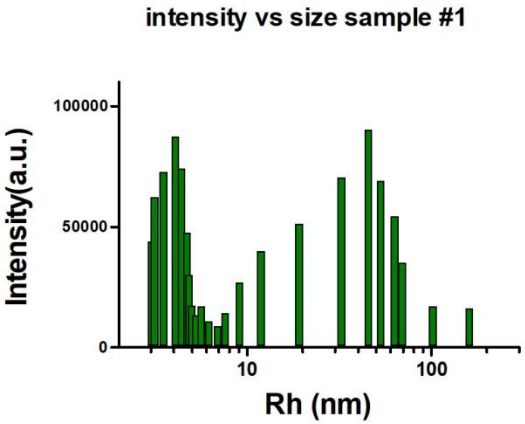
intensity vs size sample #1
Intensity(a.u.)
100000
50000
0
10
100
Rh (nm)

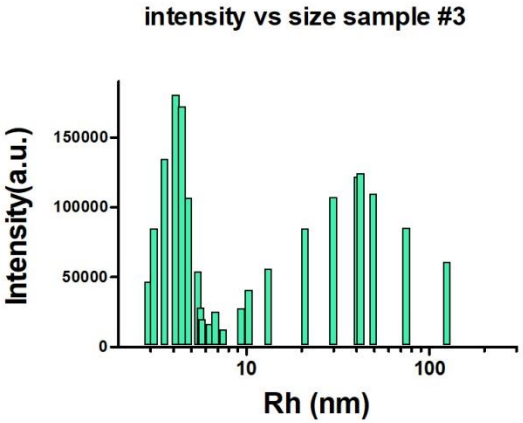
intensity vs size sample #3
Intensity(a.u.)
150000
100000
50000
0
10
100
Rh (nm)

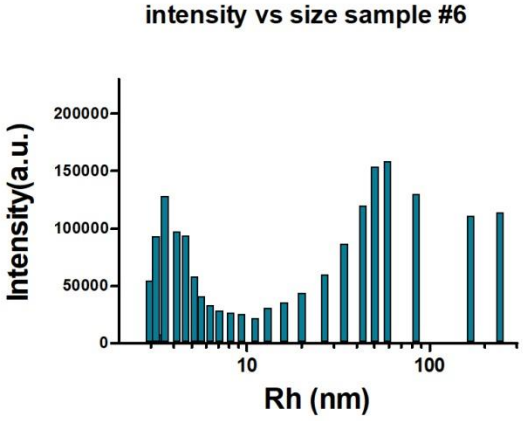
intensity vs size sample #6
Intensity(a.u.)
200000
150000
100000
50000
0
10
100
Rh (nm)

263K

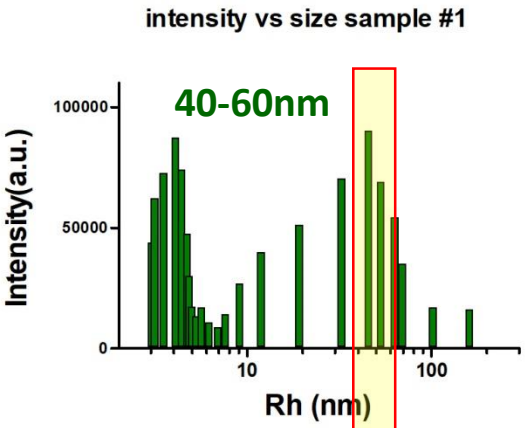
intensity vs size sample #1
40-60nm
Intensity(a.u.)
Rh (nm)

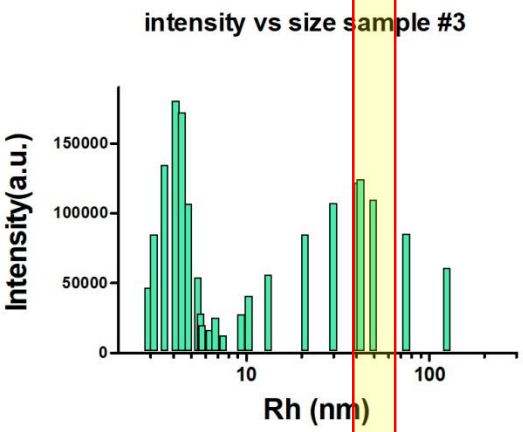
intensity vs size sample #3
Intensity(a.u.)
Rh (nm)

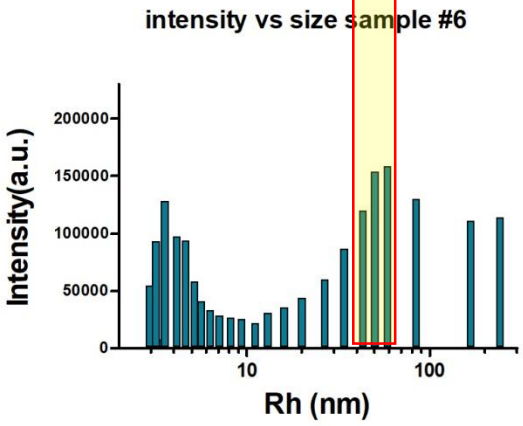
intensity vs size sample #6
Intensity(a.u.)
Rh (nm)

Hyper

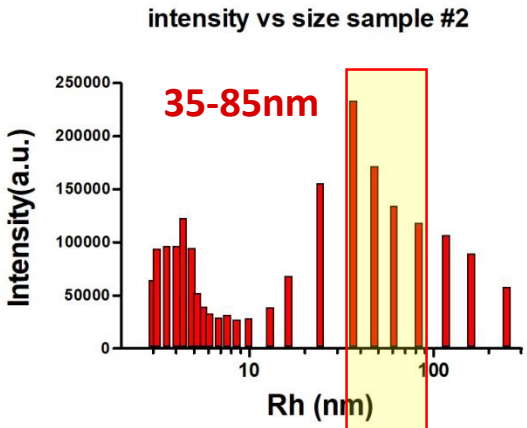
intensity vs size sample #2
35-85nm
Intensity(a.u.)
Rh (nm)

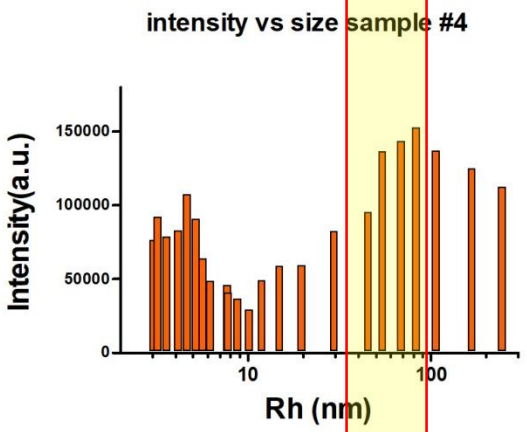
intensity vs size sample #4
Intensity(a.u.)
Rh (nm)

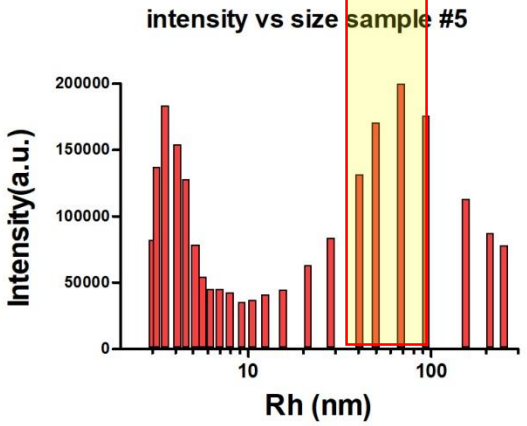
intensity vs size sample #5
Intensity(a.u.)
Rh (nm)

263K

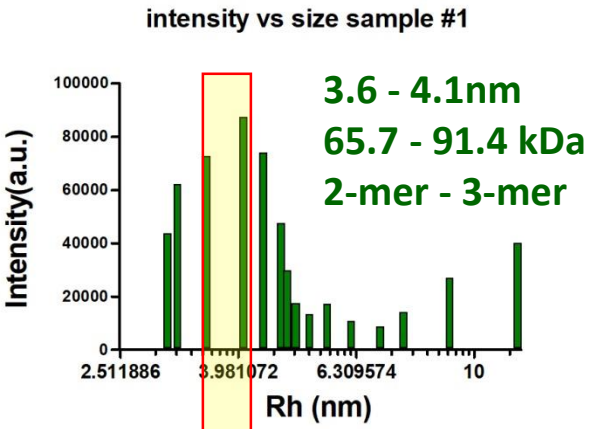
intensity vs size sample #1
3.6 - 4.1nm
65.7 - 91.4 kDa
2-mer - 3-mer
Intensity(a.u.)
100000
80000
60000
40000
20000
0
2.511886
3.981072
6.309574
10
Rh (nm)

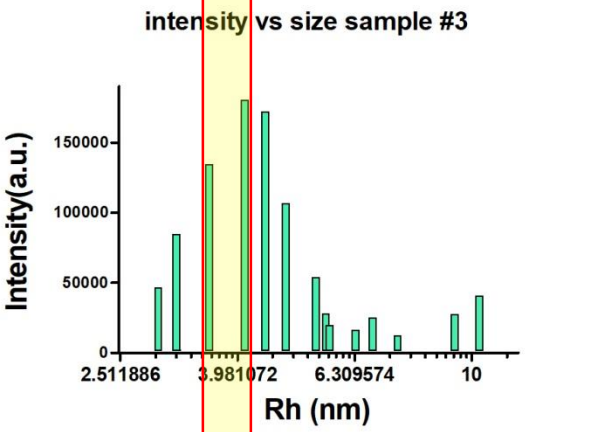
intensity vs size sample #3
Intensity(a.u.)
150000
100000
50000
0
2.511886
3.981072
6.309574
10
Rh (nm)

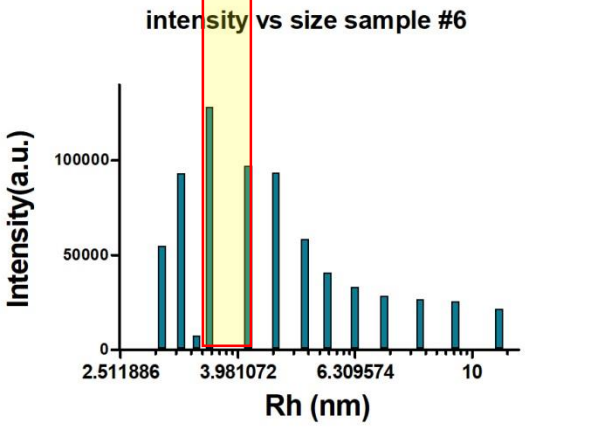
intensity vs size sample #6
Intensity(a.u.)
100000
50000
0
2.511886
3.981072
6.309574
10
Rh (nm)

Hyper

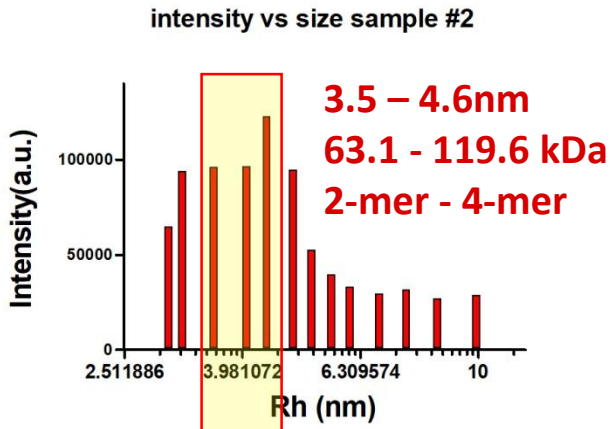
intensity vs size sample #2
3.5 – 4.6nm
63.1 - 119.6 kDa
2-mer - 4-mer
Intensity(a.u.)
100000
50000
0
2.511886
3.981072
6.309574
10
Rh (nm)

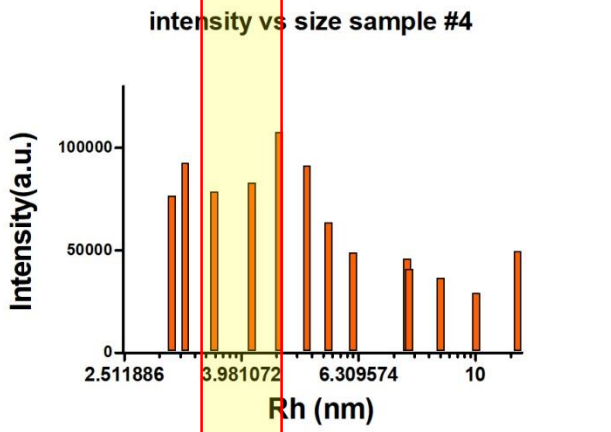
intensity vs size sample #4
Intensity(a.u.)
100000
50000
0
2.511886
3.981072
6.309574
10
Rh (nm)

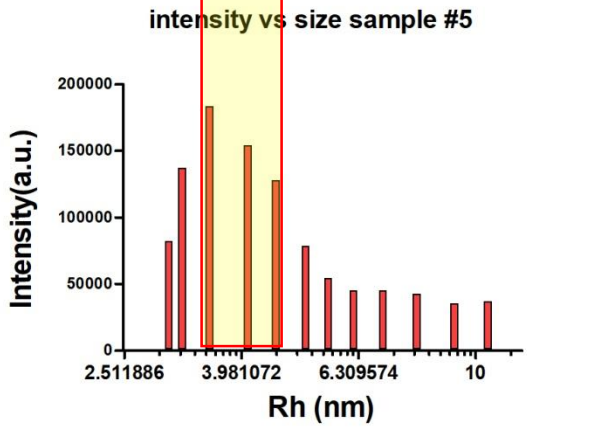
intensity vs size sample #5
Intensity(a.u.)
200000
150000
100000
50000
0
2.511886
3.981072
6.309574
10
Rh (nm)

PrP size distribution of hamster prion strains

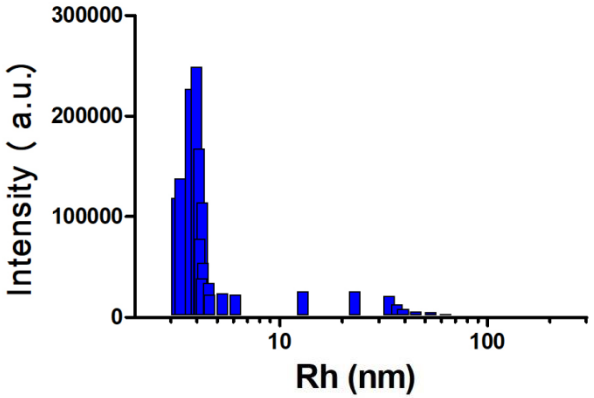

Drowsy

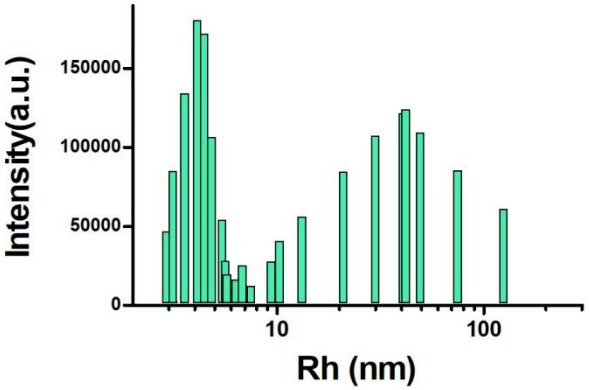

263K

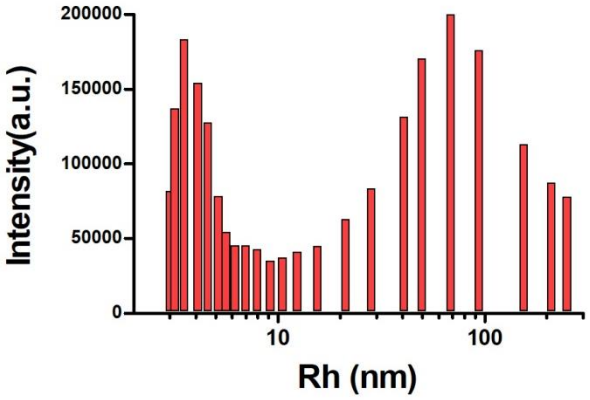

Hyper

Immunoblot - PK treated fractions

263K

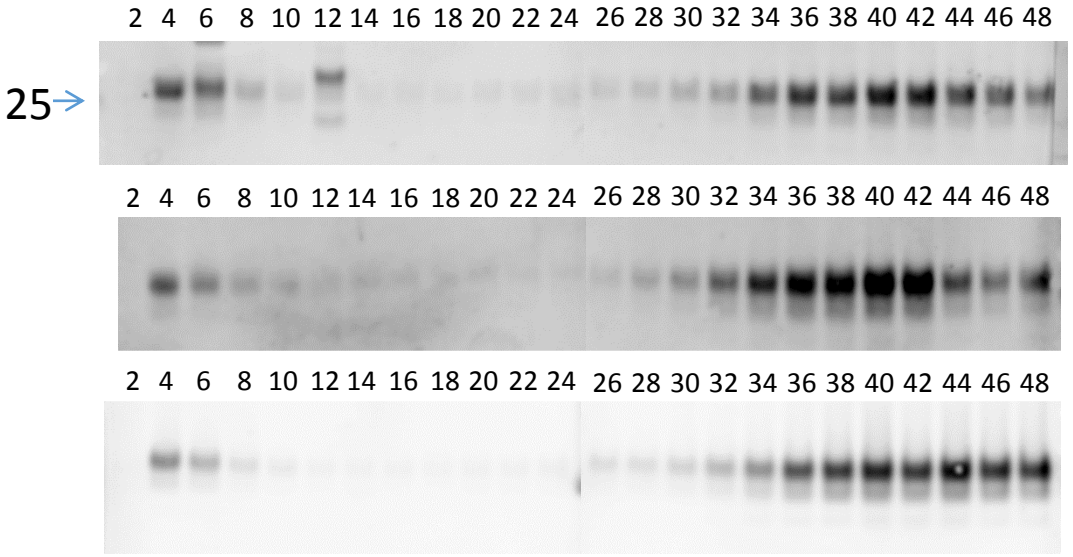

Hyper

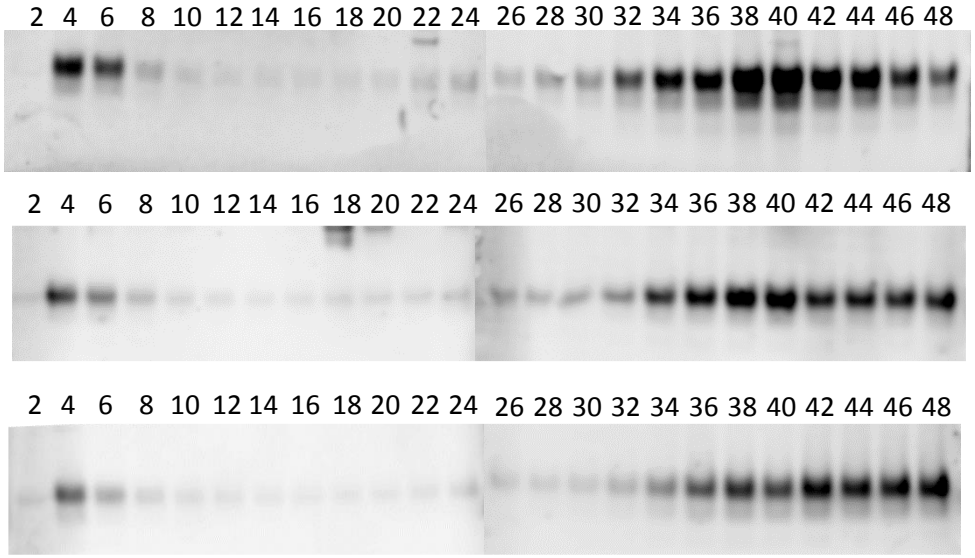

263K

Hyper

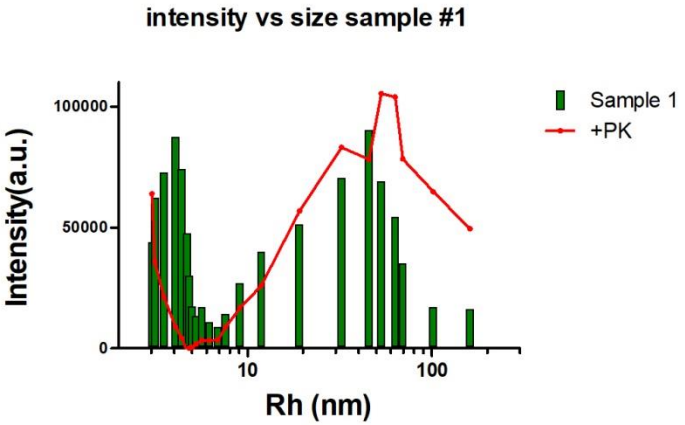
intensity vs size sample #1
Intensity(a.u.)
100000
50000
0
10
100
Rh (nm)
Sample 1
+PK

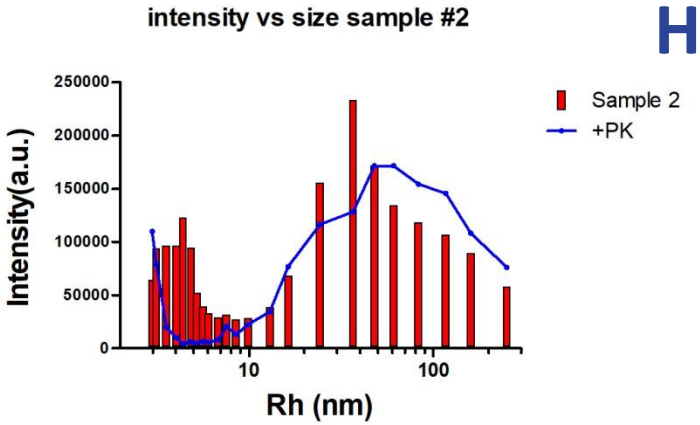
intensity vs size sample #2
Intensity(a.u.)
250000
200000
150000
100000
50000
0
10
100
Rh (nm)
Sample 2
+PK

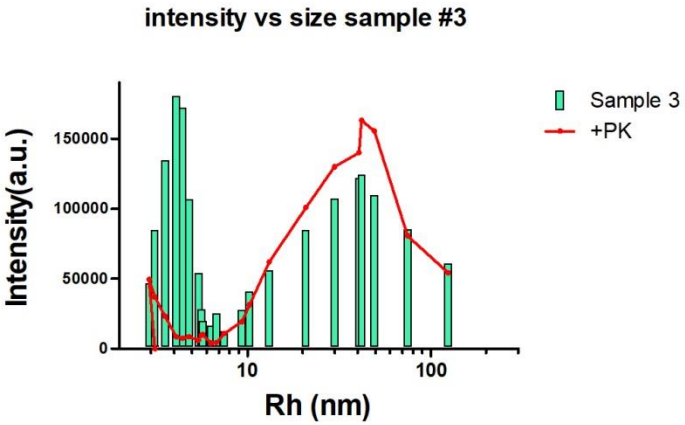
intensity vs size sample #3
Intensity(a.u.)
150000
100000
50000
0
10
100
Rh (nm)
Sample 3
+PK

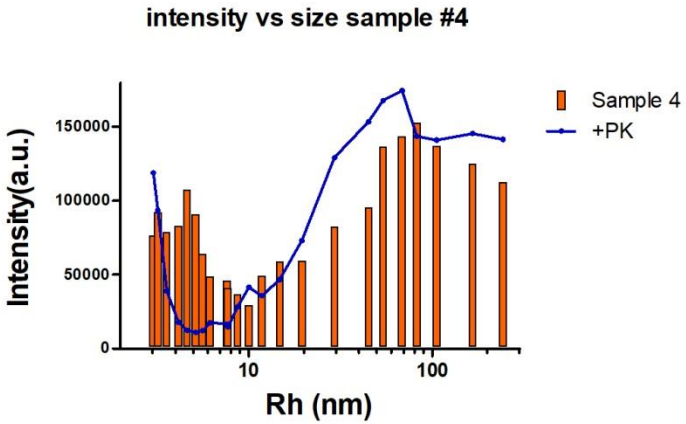
intensity vs size sample #4
Intensity(a.u.)
150000
100000
50000
0
10
100
Rh (nm)
Sample 4
+PK

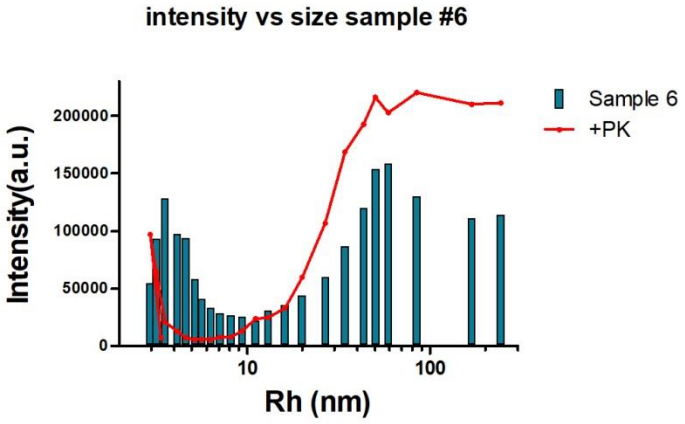
intensity vs size sample #6
Intensity(a.u.)
200000
150000
100000
50000
0
10
100
Rh (nm)
Sample 6
+PK

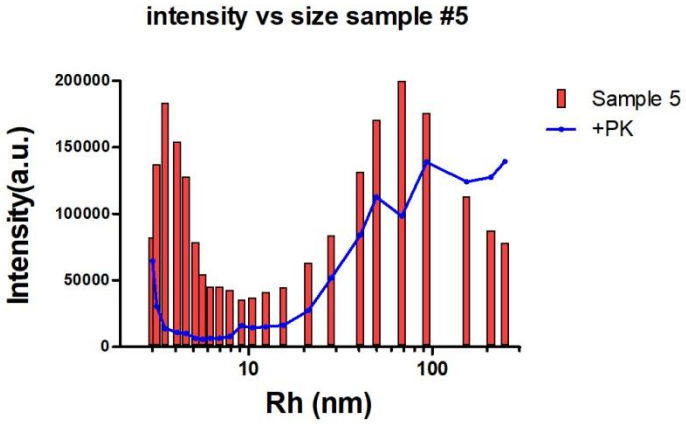
intensity vs size sample #5
Intensity(a.u.)
200000
150000
100000
50000
0
10
100
Rh (nm)
Sample 5
+PK

Evaluation of seeding activity (RT-QuIC reaction)

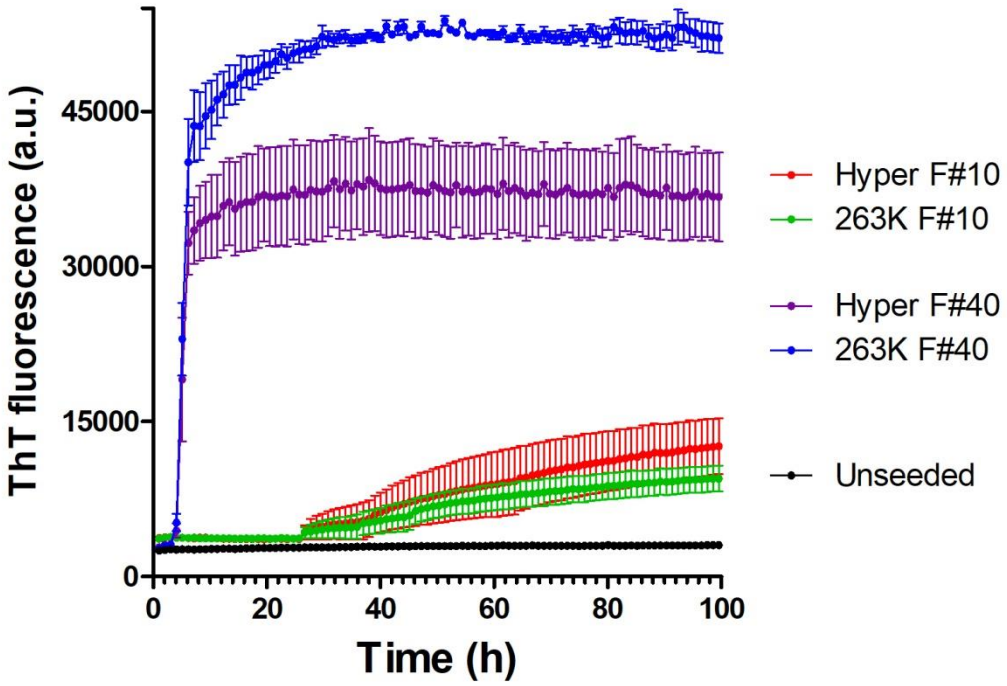

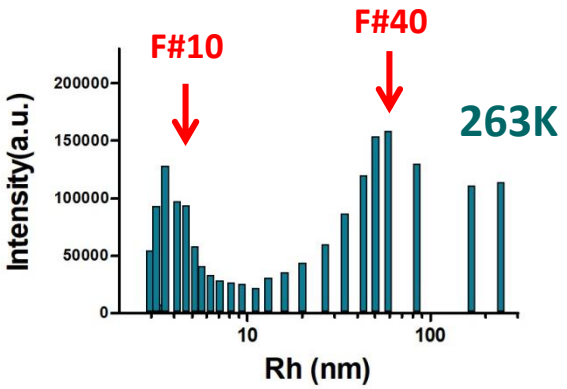

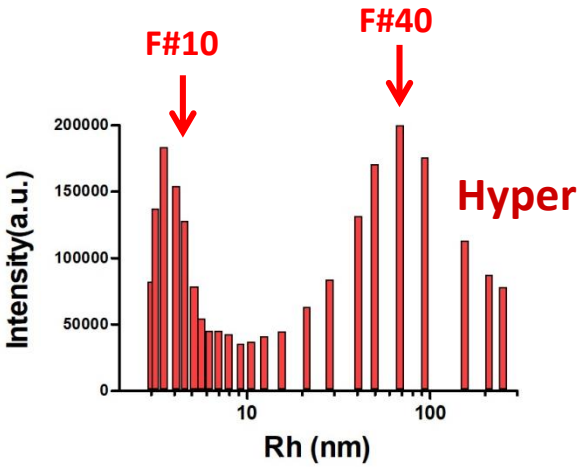

- Can we isolate the different prion particles present in brains at terminal stage of prion disease? ✓
- Are different strains composed by different cloud of prion particles? ✓
- Can we characterize the prion particles present in these clouds and identify the most pathogenic prions? ✓
- Are these pathogenic particles strain-specific?

Identifying the most pathogenic prion particles in CJD is vital to our understanding of prion disease in humans. Such knowledge will address the fundamental question of how human prion particles induce pathology and will inform therapeutic strategies to combat the disease.

Future Directions

→ Compare strains using different AF4 running conditions to get better resolution at small R_H particles

→ Measure infectivity of the isolated prion particles (cell culture and animal experiments)

→ Compare mouse-adapted CJD strains (sCJD cortex, fCJD cerebellum, GSS cerebellum)

→ Analyze human brains of patients with the following strains of CJD:

sCJD (129MM, MV, VV),
fCJD (E200K),
vCJD,
GSS (A117V, Q227Vstop, 5 and 7 octapeptide repeat insertions),
FFI (D178N),
sFI

Acknowledgement

Valerie Sim's Lab

Grant Norman
Hailey Pineau
Helen Yao

Debbie McKenzie's Lab

Camilo Duque-Velasquez
Jacques Van der Merwe

Holger Wille's Lab

Claudia Acevedo-Morantes
Brian Tancowny

CENTRE FOR PRIONS
AND PROTEIN FOLDING DISEASES

UNIVERSITY OF ALBERTA

The **Christopher "Dutch" Grammel and Michael Roll Memorial Grant**, contributed by Scott and Beth Grammel

The "**Mercies in Disguise Grant in Honor of the Baxley Family**," contributed by Kathy Baxley and Family

The **José A. Piriz and Sonia E. Piriz Memorial Grant**, contributed by Karla Piriz and Lauren Piriz

The **Patrick Yobs Memorial Grant**, contributed by Debbie Yobs and Family

The **Strides for CJD Grant**, contributed by the Families of the CJD Foundation

CJD FOUNDATION

CREUTZFELDT-JAKOB DISEASE FOUNDATION, INC.

Supporting Families Affected by Prion Disease

SUMMARY

Introduction:

Human prion diseases are fatal, progressive neurodegenerative conditions characterized by the accumulation of aggregated forms of the prion protein (PrP^{C}) into a variety of aberrant structures (PrP^{Sc}). These aberrant aggregates range in size from very small to very large particles. Little is known about which of these particles are the most pathogenic and ***potential targets for therapeutic intervention*** in CJD.

In addition, the existence of different strains of human CJD, which differ in clinical presentation, PrP^{Sc} biochemistry and patterns of PrP^{Sc} deposition in brain, add more complexity to the finding of an effective treatment. It is theorized that each prion strain consists of a specific group or "cloud" of PrP^{Sc} aggregates.

Goals:

In this study, we are analyzing the composition of these "clouds" by isolating their components (the different PrP^{Sc} aggregates present in these clouds) and measuring their properties (size, amount, stability, seeding activity, infectivity, etc.) in order to find the strain-specific pathogenic prion particles.

Methods:

As source of prions we are using mouse, hamster and human brains infected with different prion strains at terminal stage. The brain tissue is mechanically homogenized in presence of detergents to dissolve their components. These components are then separated using a technique called Asymmetric-Flow Field-Flow Fractionation (AF4). Once isolated we start the characterization of these prion particles.

Results:

We found that the composition of the prion "clouds" vary between strains.

We also found common features between all the analyzed "clouds" since two main populations of PrP^{Sc} particles were found in all the studied strains:

- Small particles with low capacity to generate new prions (low seeding activity) and low resistance to action of proteases.
- Big particles with high seeding activity and resistant to the action of proteases.

We are also studying how the composition of the prion "cloud" evolves during the curse of prion infection. To do so, we culture prion infected mouse brain tissue; we harvest aliquots of this tissue every week and then analyze these aliquots in the same way that we analyzed the brain homogenates in our previous experiments.